Chapter 5

Lab-on-a-Tube Surface Micromachining Technology

Zhuoqing Yang and Yi Zhang

Additional information is available at the end of the chapter

http://dx.doi.org/10.5772/66664

Abstract

In this chapter, the lab-on-a-tube surface micromachining technology will be used to fabricate a flexible implantable microtemperature sensor for hyperthermia application and a three-electrode system on a polymer tube surface for glucose monitoring application. This micromachining process is based on two homemade equipments: a spray coating equipment and a programmable UV 3D projection lithography system with alignment. In the spray coating system, there is a heater nozzle next to the spray nozzle for real-time heating. Pure nitrogen is flowed through the heater nozzle, warmed up and sprayed onto the tube substrate surface. The programmable UV lithography equipment for cylindrical substrate mainly consists of four parts: a uniform illumination system, a reduced projection lithography system, a synchronized motion stage system, and a Charge-Coupled Device (CCD) multilayer alignment system which is used to observe simultaneously the projected mask's patterns and those ever fabricated on the tube. Using the developed lab-on-a-tube surface micromachining technology, an implantable flexible microtemperature sensor and a three-electrode microstructure are successfully fabricated on the flexible polymer tube with 330 μm outer diameter, respectively. The test temperature coefficient of resistance (TCR) of the temperature sensor is 0.0034/°C. The measured cyclic voltammetry curve shows that the three-electrode system has a good redox property.

Keywords: micromachining, lab-on-a-tube, thin film, flexible cylindrical substrate, 3D lithography

1. Introduction

With the development of the Internet of Things (IoT), wearable devices, and implantable biomedical components, the flexible sensors, actuators, and electrical circuits have been demanded more and more widely. However, the traditional silicon-based surface micromachining technologies are difficult to meet this requirement due to natural brittle structure. With regard to this, we developed a novel micromachining method that mainly includes

spray coating, lithography pattering, and multilayer alignment on the flexible cylindrical substrate, such as fiber, polymer tube, capillary, and other tubes. It can realize the integrated fabrication of many sensors and actuators with different functional materials on an ultrathin (hundreds of micrometers) flexible cylindrical substrate, which is very promising to wearable devices and biomedical applications in the future. Here, we called it "lab-on-a-tube surface micromachining technology."

In this chapter, the equipments used for lab-on-a-tube surface micromachining will be described in detail. Firstly, a spray coating system for cylindrical substrate will be introduced, and the effect of process parameters on the quality of the coated photoresist (PR) film on tube surface will be also discussed. Then, the UV projection lithography system for cylindrical substrate is developed, and its working principle is described in detail. Finally, two application examples of the developed lab-on-a-tube surface micromachining technology will be shown, one is the flexible implantable microtemperature sensor on a polymer tube surface, another is flexible implantable microneedle with three-electrode system for glucose sensor.

2. Equipments for lab-on-a-tube surface micromachining

2.1. Spray coating system for cylindrical substrate

A homemade equipment was built, as shown in **Figure 1**, which can realize the spray coating of PR film on the tube surface. In order to complete real-time heating for the tube with coated film, a heater nozzle was used, where nitrogen gas (N_2) will be flowed. The temperature of N_2 gas was controlled by using two temperature sensors at the inside and outlet of the heater nozzle. The scan speed of the spraying nozzle, the rotation speed of the tube, and the distance between spray nozzle and the tube can be all independently controlled. They are main process parameters in the current system [1].

In the present work, the photoresist (PR) solution including a positive photoresist S1830 and a thinner AZ 5200 was used as the PR film coated on the tube surface. In the solution, their weight ratio is 1:1. **Figure 2** shows the effect of the nozzle/tube distance on the thickness of coated PR film when using the real-time heating or not. **Figure 3** is the measured variations of the PR film thickness versus the rotation speed when using different weight ratios and

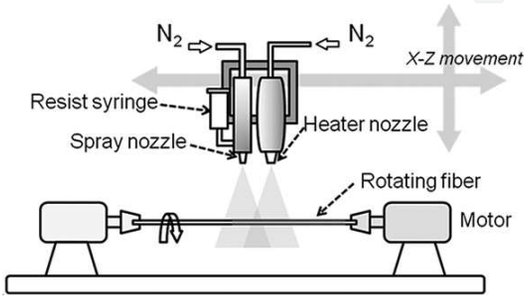

Figure 1. Homemade spray coating system for tube substrate and its schematic setup [3].

http://dx.doi.org/10.5772/66664

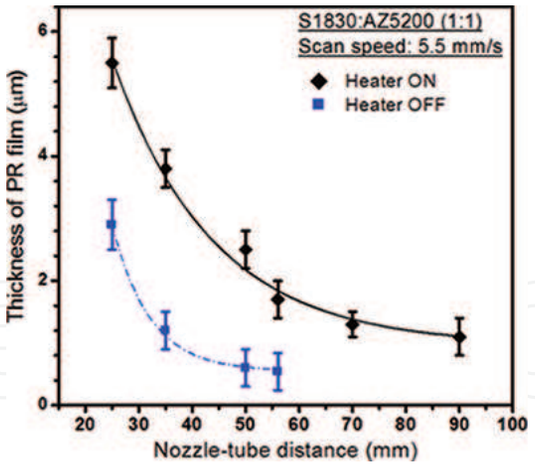

Figure 2. Measured effects of the real-time heating process on the variation of the PR film thickness versus the nozzle tube distance.

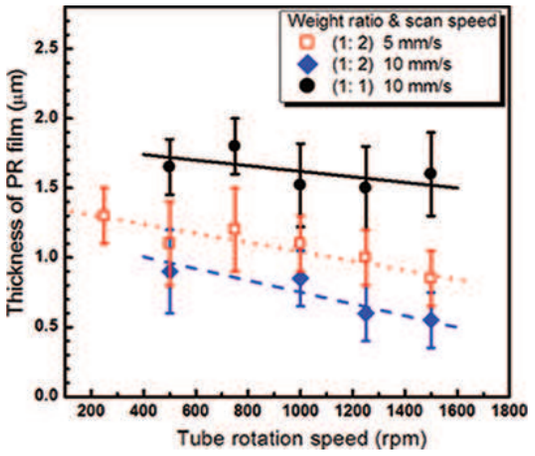

Figure 3. Measured variations of the PR film thickness versus the rotation speed under different weight ratios and cycle scanning speeds.

cycle scanning speeds. It can be found that the quality of the coated PR films is not good if there is no real-time heating during spray coating. The thinner PR film would be obtained if increasing the rotation speed and thinner concentration. Because that the centrifugal force will become larger when the rotation speed of the tube increases. So PR solution particles will be thrown away more from the tube surface. Finally, the PR films become thinner when increasing the rotation speed.

These experimental results about the spraying PR film on the tube surface are generally in accordance with the previous reports [1, 2]. However, considering the size of tube is very small compared to those of the spray jet and the nozzle/tube distance. So its basic principle is different from the traditional coating process, where the size of wafer is usually planar shape with several inches. A so-called impinging region existing below the nozzle will cover the tube spraying area. Moreover, considering the spraying PR particles (about 10–20 μm) is usually only one-tenth of the tube diameter, the influence of the rotation speed is more obvious than the real-time heating during the spray coating. Especially for that using low-volatility

thinner, the real-time heating is more important. Otherwise, it is difficult to obtain continuous and smooth PR film surface. In addition, the effect of process parameters in the spray coating on the quality of PR film on tube surface has been fully studied in our previous work [3, 4].

2.2. UV projection lithography system for cylindrical substrate

Figure 4 shows the sketch of the developed UV lithography system for tube surface. The whole system mainly consists of four units: a synchronized motion stage, a reduced projection exposure unit, a CCD multilayer alignment part, and a uniform illumination unit. After through a reduced mask image, the UV light used as exposure source will be focused onto the bottom surface of the tube with coated PR film. The wavelength of the used UV light is 250–600 nm. With regard to this, a 436 ± 10 nm interference filter was used to eliminate the aberration. Finally, the magnifying power of the objective lens will determine the amplification factor of the whole lithography system. In the present work, the overall reduced factor is 0.5 when the pattern of mask is transferred to the surface of the tube. This is reasonable and enough for our current research. By the abovementioned setting, a focal depth of ±45 μm can be realized in the developed UV lithography system that will be used to exposure and patterning the tube surface with coated PR film. Two chucks in the rotation stages are used to fix the tube in order to make sure the coaxial rotation. In addition, for adjusting the coaxiality conveniently, a laser was also used as a reference.

The final whole lithography system that includes five degrees of freedom (DOFs) is shown in **Figure 5(a)**. The patterns on mask and tube can be seen simultaneously by using two CCD, which can help to complete the secondary or multilayer alignment in the exposure. The side

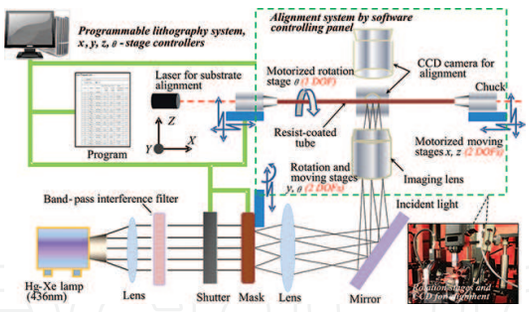

Figure 4. Schematic illustration of programmable UV lithography system with alignment for cylindrical substrates [4].

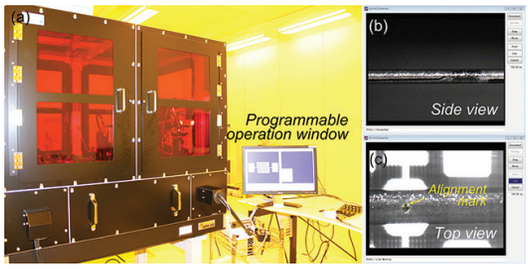

Figure 5. Optical photo of (a) final developed lithography equipment and CCD for alignment and (b) side view and (c) top view in the programmable operation window.

http://dx.doi.org/10.5772/66664

view and top view in the programmable operation window are shown in **Figure 5(b)** and **(c)**, respectively. The programmable software can automatically control motorized XYZ-θ stages and exposure time. The movement and the rotation accuracies are 0.1 μm and 0.01° in the axial direction and the θ-direction, respectively. By using PC operation window and doing those programmable sentences, the PR film on the tube surface can be patterned according to the design. Finally, the PR patterns with expected microstructures will be obtained on the tube surface after the development. This equipment can be used not only for tube exposure but also for those similar cylindrical substrates, such as optical fibers, capillary, metal or fabric wires, etc. The working principle of the developed lithography system can be found in our previous works [4, 5].

Micropatterning on the tube surface can be easily realized by using the developed programmable lithography equipment. Firstly, you can decompose the designed pattern into sequential programmable sentences in the PC operation window. Then, the software will automatically control the movements of stage, mask, and tube; the UV light will complete the exposure to the tube surface with coated PR film according to the programmable sentences. For example, you can complete an oblique line pattern on the tube by controlling the tube to parallel translation and rotate simultaneously. Of course, the final angle of the oblique line will be determined together by their two speed values in the respective directions. In the exposure, we can conveniently tune the intensity by changing the quantity of projection light and movement speed of the tube. **Figure 6** is the preview patterns of some microstructures after completing the programmable sentences, such as (a) micro-heater and (b) resonator. These micropatterns will be firstly drawn by programmable operation window in our developed lithography system shown in **Figure 5**. Then, they will be fabricated on the silica glass tube surface. After the exposure of these cylindrical tubes with coated PR film by the above programmable lithography system, the development was carried out subsequently. As a result, the PR films on the tube surfaces have been successfully patterned as those expected program patterns in **Figure 6(a)** and **(b)**, which are as shown in **Figure 6**(**a**′) and (**b**′).

After sputtering Pt film and subsequent lift-off process, the two kinds of microstructures are clearly seen, including zigzag micro-heater and partial patterns of resonator, which are

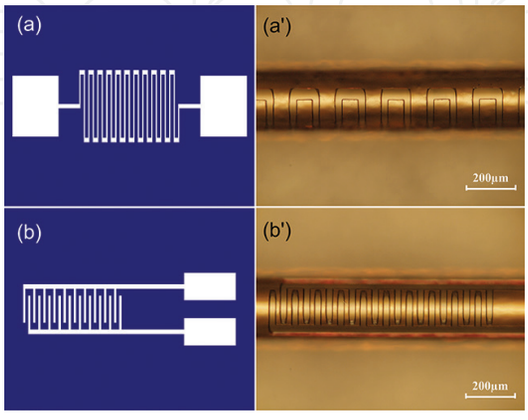

Figure 6. Planar previews of the programmed (a) micro-heater and (b) resonator patterns and (a′–b′) obtained micropatterns on silica glass tube after exposure and development according to corresponding programmed patterns.

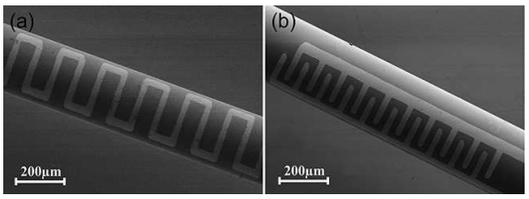

Figure 7. SEM of fabricated (a) zigzag structures of micro-heater and (b) resonator.

shown in **Figure 6** (**a**′) and (**b**′). **Figure 7** shows the Scanning Electron Microscope (SEMs) of these microstructures. The PR film thickness and the line width are ~2 and 20 μm, respectively. As so far, the line width of 10 μm has been obtained by using special fabrication process in our developed lithography system.

3. Application examples

3.1. Flexible implantable microtemperature sensor

The hyperthermia is still considered as an effective way for the cancer treatment, which has been proven in many clinical studies. In the treatment, the microwave was used to heat the lesion to above 42°C in order to kill tumors. At the same time, we have to make sure the normal tissue not to be damaged [6]. So, in the hyperthermia it is necessary to develop a microtemperature sensor for measuring the temperature precisely. Although many researchers have fabricated some microtemperature sensors, they cannot be used as a flexible device to implant into the objects due to its fabrication based on silicon process [6–8]. Its natural brittle feature is not beneficial. Therefore, some researchers try to develop thinner sensor based on the cylindrical substrate in order to implant into the tissue. For example, a microcoil on the capillary surface for magnetic resonance imaging (MRI) interventional treatment has been reported in Ref. [9]. Similarly, in Refs. [10, 11], a radio frequency (RF) coil has also been developed on the cylindrical surface for portable nuclear magnetic resonance (NMR) diagnosis. In addition, the soft lithography technology was used to realize patterning on the curved surface in Ref. [12]. Even, in order to fabricate microstructures on the thin cylindrical substrate, an automatic wire bonder was also utilized in the work [13, 14]. However, in these methods the devices are usually fabricated on glass capillary or metal stick surface. The whole flexibility of the sensor is poor, and corresponding fabrication resolution and sensitivity are neither not good. In addition, in these methods only one kind of material can be used and fabricated because the multilayer alignment cannot be realized. As a result, their applications have been subjected to a lot of limitations.

In the present work, using the developed programmable UV lithography system, a flexible implantable microtemperature sensor for hyperthermia application will be designed and fabricated. Finally, the fabricated microtemperature sensor will be also evaluated in detail.

In this work, we design a flexible implantable microtemperature sensor on a polymer tube with only 330 μm outer diameter for hyperthermia application. This sensor will be fabricated

http://dx.doi.org/10.5772/66664

using the above developed lithography system. The design sketch of the temperature sensor and its corresponding general working principle is shown in **Figure 8(a)**. In the future practical application, you can implant the part of the sensor into the tumor and monitor its temperature. The doctor can make a right decision and precise operation by referring the measured result from the microtemperature sensor. The material of the sensing element in the sensor is platinum (Pt) considering its good resistance-temperature effect. The sensing element and its geometric parameters are shown in **Figure 8(b)** and **(c)**, respectively.

ANSYS was used to do the simulation of the microtemperature sensor. **Figure 9** is the 2D model of the sensor, which only contains one Pt line and pitch unit because of its symmetry. The polymer tube from Furukawa Electric Co., Ltd. was used as the substrate because of its excellent physical and chemical stabilities. It is substantially a kind of commercial polyimide (PI) material. Especially, this tube can withstand the temperature up to 200°C. Before simulation the related boundary conditions need to be determined according to application environment. The temperature of tube surface was set as 37°C, which was considered as the normal tissue. Here, 42°C is set as the highest temperature in the hyperthermia. The transient simulation was carried out for dynamic response of the designed microtemperature sensor. **Figure 9(b)–(g)** shows the simulated results. It can be seen that the temperature didn't continue to spread along the vertical direction of the tube surface until the moment about 2–4 ms, which means the response time of the sensor.

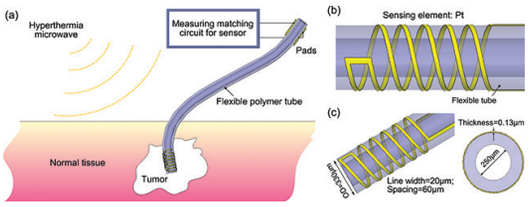

Figure 8. (a) Sketch of the flexible microtemperature sensor on the polymer tube for hyperthermia, (b) sensing element, and (c) its structural parameters [4].

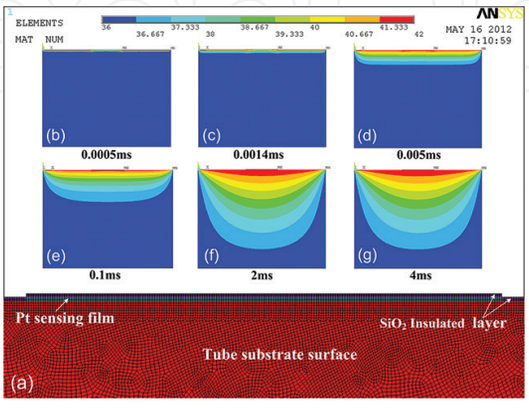

Figure 9. Dynamic simulation of microtemperature sensor used in hyperthermia. (a) FE model and (b)–(g) transient temperature field distributions [4].

The general fabrication process of the temperature sensor is described in **Figure 10**, as follows:

a. Cleaning the polymer tube. Using a UV ozone treatment unit (VX-0200HK-002, ACingTec, Japan) to clean the surface and modification.

b. Spray coating ~2.5 μm PR on the tube substrate by developed homemade coating system.

c. Exposure and patterning of the polymer tube with coated PR film by developed cylindrical lithography method.

d. Magnetron sputtering Pt film (~0.13 μm) onto the patterned tube surface.

e. PR film was removed by lift-off.

f. Again spray coating PR film (~2 μm) on the tube with patterned Pt microstructures.

g. Secondary exposure and development were done to pattern the PR film again.

h. SiO_2 layer ~0.3 μm was deposited on the Pt film for electric isolation.

i. Obtaining the microtemperature sensor after removing the residual PR film by acetone solution. The detailed fabrication process steps of the sensor can be found in our previous report [15].

The polymer tube substrates used in this work were all cleaned by immersing in the H_2SiO_4/H_2O_2 solution at 115°C for 15 min and then rinsed with purified water. The PR film was depositing on the tube surface by homemade spray coating setup. During the spray coating, the real-time heating was used always. The thickness of coated PR film can be controlled by cycle spray coating number and tube rotation speed. In the fabrication of Pt sensing element in the

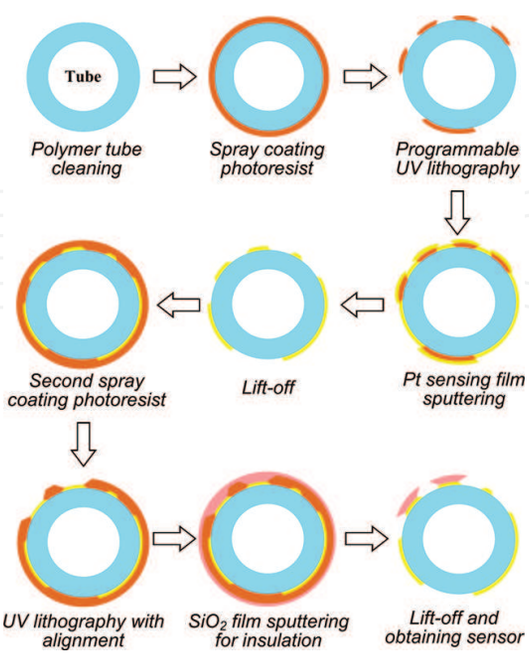

Figure 10. Main fabrication processes of flexible microtemperature sensor on the polymer tube.

http://dx.doi.org/10.5772/66664

sensor, the quality of the Pt film is very important considering it is used as the critical sensitive material. The sputtering condition is the vacuum 7.0×10^{-4} Pa, the purity of Ar gas 99.9%, the purity of Pt target 99.99%, and sputtering power 100 W. The fabrication process steps of the microtemperature sensor are described in our previous work [15].

The optical photo of the final fabricated flexible microtemperature sensor is shown in **Figure 11**. It can be seen that the sensor has a good flexibility. The Pt sensing element in the sensor can be also seen clearly in the right picture in the figure. Also, the line patterns of the fabricated sensing element on the polymer tube are clearly shown in **Figure 12**.

Platinum (Pt) film temperature sensing will experience a change in resistance with environmental temperature according to the following formula:

$$R_t = R_0\left[1 + \alpha\left(T - T_0\right)\right] \tag{1}$$

where R_t is the resistance at the working temperature T and R_0 is the resistance at the reference temperature T_0. And, α is the temperature coefficient of resistance (TCR). By slowly increasing and reducing the temperature from room temperature to 90°C, we can obtain the TCR, as shown in **Figure 13**. It is generally 0.0034/°C. This measured value is lower than the theoretical value of bulk pure Pt (0.0039/°C) because the electron scattering would be cause grain not be density during the film sputtering [16]. Of course, the deviation will also be caused by fabrication parameters, testing method, etc.

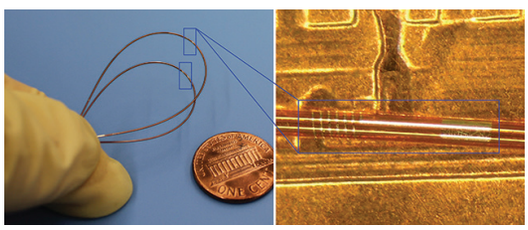

Figure 11. Optical photo of the fabricated flexible microtemperature sensor next to a coin for reference and its sensing element micropattern.

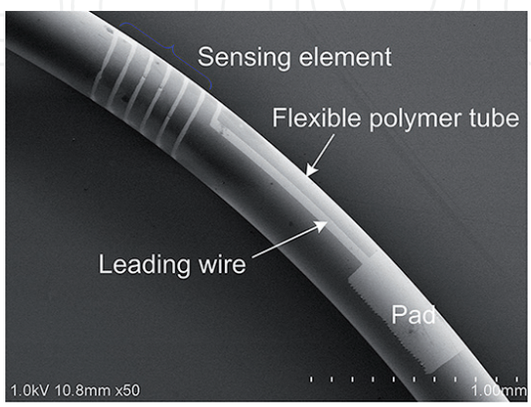

Figure 12. SEM photograph of the fabricated flexible microtemperature sensor on polymer tube surface.

3.2. Flexible implantable microneedle with three-electrode system for glucose sensor

As another example of the developed programmable UV lithography system, a three-electrode system will be designed and fabricated on a polymer tube surface. As a result, the tube with three-electrode microstructure can be used as a flexible microneedle, which could be promising in the implantable glucose sensor for human body in the future. **Figure 14(a)** is the sketch of the designed system and its configuration. The one end of the microneedle can be used as an implantable sensor considering its flexibility and thin size. In addition, the hollow structure of the tube may be as a convenient path for potential drug delivery. The three-electrode structure is as follows: counter electrode (CE), reference electrode (RE), and working electrode (WE). **Figure 14(b)** and **(c)** shows the corresponding geometric parameters and configurations. Some external measuring and controlling systems are also necessary if the microneedle would be used in the glucose monitoring and insulin injecting.

Figure 15 generally describes fabrication steps of the three-electrode structure on the polymer tube, as follows:

a. Polymer tube substrate ready and cleaning the surface of the tube using plasma.

b. Spray coating PR film ~2 μm on the polymer tube surface by developed spray coating system.

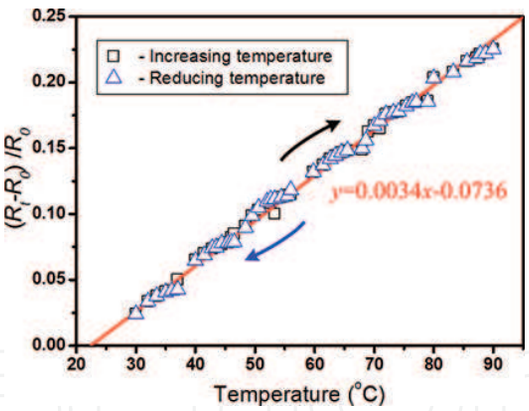

Figure 13. Test TCR of the flexible microtemperature sensor fabricated on the polymer tube surface.

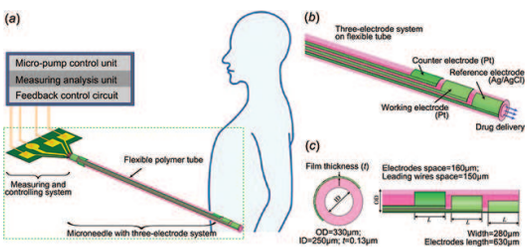

Figure 14. (a) Sketch of the interventional flexible implantable microneedle with three-electrode system for continuous glucose monitoring and drug delivery, (b) distributions, and (c) main structural parameters [17].

c. Patterning the tube with coated PR film according to the programmable micropattern of three-electrode pattern using the developed programmable UV lithography equipment.

d. Magnetron sputtering of 120 nm thick Pt film onto the tube surface with patterned PR. Lift off and remove the residual PR and obtaining three-electrode patterns.

e. The second spray coating PR and lithography with alignment.

f. Sputtering Ag layer and AgCl layer preparation; remove residual PR film by lift-off process. Finally, the three-electrode pattern was completed. The detailed fabrication process steps of the microneedle can be found in our previous reports [17, 18].

In the above fabrication of the three-electrode structure, the Ag/AgCl electrode must be completed according to programmable patterns as shown in **Figure 16**. In addition, the second lithography with alignment in the experiment is very critical. The related operation can be found in our previous work [17]. **Figure 16** shows the programmable micropattern of the three-electrode system (left) and the three-electrode structure obtained by programmable lithography equipment with multilayer alignment: PR boundaries in −40° and −10° views after the development by secondary alignment (right). So far, we have realized the ±1 μm alignment precision using the developed lithography system.

Figure 17 is the final fabricated three-electrode structure on the polymer tube surface. The whole structure can be used as an implantable flexible microneedle because of its good flexibility property. Generally, this proposed device shows better overall property than other similar reports [19–24]. The novel design including a three-electrode structure on a thin hollow tube will be very useful for some applications in the micro-total analysis systems (μTAS) in the future.

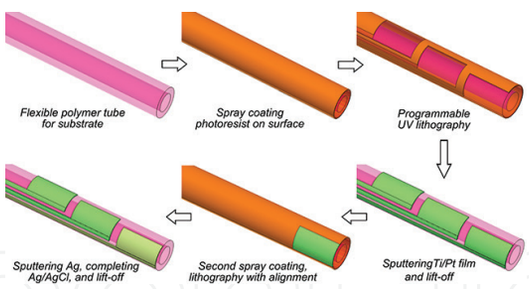

Figure 15. Main fabrication process of the three-electrode structure in flexible microneedle on polymer tube surface.

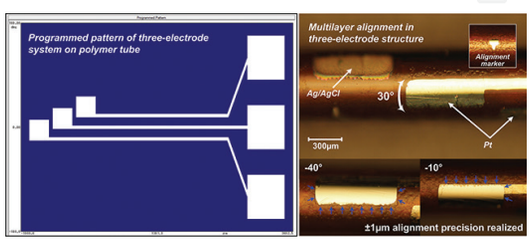

Figure 16. Programmable micropattern of the three-electrode system (left) and three-electrode structure obtained by programmable lithography equipment with multilayer alignment: PR boundaries in −40° and −10° views after the development by secondary alignment (right).

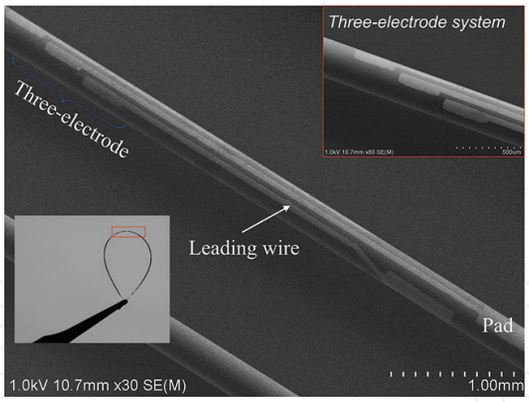

Figure 17. SEM and optical photo of the fabricated three-electrode system on a polymer tube surface as a flexible microneedle.

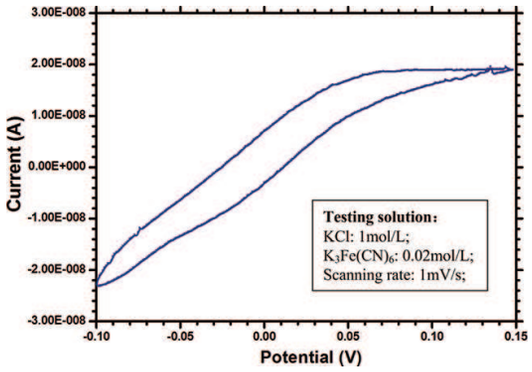

Figure 18. Measured cyclic voltammetry curve of the three-electrode pattern on the fabricated prototype microneedle on polymer tube surface.

Next, the fundamental electrochemical property of the fabricated three-electrode structure was measured. The detailed measuring method, conditions, and related equipment used can be found in our previous work [17]. The measured cyclic voltammetry (CV) curve is shown in **Figure 18**. It indicates the device has a good redox property. But the peak of the test current is not very evident. Very small reaction area in the three-electrode pattern is considered as a main reason because of thin tube diameter. In addition, the quality of the sputtering Pt film is another affected factor. We can obtain an estimated peak current density according to the above measured result, about 0.8 mA/dm^2, which is sufficient for subsequent circuit signal processing in the glucose sensor application. In addition, our fabricated flexible microneedle device can be more easily implanted into the objects compared to other reported ones [23–26].

4. Conclusion

In this chapter, a lab-on-a-tube surface micromachining technology for cylindrical substrates has been built for the first time based on the developed programmable UV lithography system with alignment. The related equipments used in the lab-on-a-tube surface micromachining,

including a homemade spray coating system and a projection exposure system for cylindrical substrate, have been introduced, and corresponding working principle and process parameters have been also explained. Then, as the application examples, an implantable flexible microtemperature sensor and an implantable microneedle with integrated three-electrode system on the tube surfaces have been proposed, fabricated, and characterized. The magnetron sputtering Pt film is used as the sensing material in the temperature sensor. The test TCR of the fabricated sensor is 0.0034/°C. The fabricated three-electrode structure on the polymer tube in CV measurement shows a good performance. The developed microneedle with the integrated three-electrode pattern will be very promising in the implantable glucose sensor for the human body in the future.

Acknowledgements

The authors would like to express their gratitude for the support from the National Natural Science Foundation of China (No. 61571287), Hi-Tech Research and Development Program of China (2015AA042701), Shanghai Pujiang Program (14PJ1405800), and Japan Society for the Promotion of Science (JSPS).

Author details

Zhuoqing Yang[1] and Yi Zhang[2]*

*Address all correspondence to: yi.zhang@aist.go.jp

1 Shanghai Jiao Tong University (SJTU), China

2 National Institute of Advanced Industrial Science and Technology (AIST), Japan

References

[1] N. P. Pham, J. N. Burghartz and P. M. Sarro, "Spray coating of photoresist for pattern transfer on high topography surfaces," *J. Micromech. Microeng.*, vol. 15, pp. 691–697, 2005.

[2] V. K. Singh, M. Sasaki, K. Hane, Y. Watanabe, H. Takamatsu, M. Kawakita and H. Hayashi, "Deposition of thin and uniform photoresist on three-dimensional structures using fast flow in spray coating," *J. Micromech. Microeng.*, vol. 15, pp. 2239–2345, 2005.

[3] Y. Lu, Y. Zhang, J. Lu, A. Mimura, S. Matsumoto and T. Itoh, "Three-dimensional photolithography technology for fiber substrate by using microfabricated exposure module," *J. Micromech. Microeng.*, vol. 20, 125013(10pp), 2010.

[4] Z. Yang, Y. Zhang, T. Itoh and R. Maeda, "Flexible implantable microtemperature sensor fabricated on polymer capillary by programmable UV lithography with multilayer alignment for biomedical applications," *J. Microelectromech. Syst.*, vol. 23, no. 1, pp. 21–29, 2014.

[5] Z. Yang, S. Liu, F. Xue, Y. Zhang, X. Zhao, J. Miao and L. K. Norford. "Micro anemometer by a MEMS compatible lab-on-a-tube technology", *18th International Conference on Solid-State Sensors Actuators and Microsystems* (*TRANSDUCERS 2015*), 2015.

[6] L. Lin, Q. Pei, J. Xu and H. Guo, "A microfabricated temperature sensor for hyperthermia," in *5th IEEE International Conference on Nano/Micro Engineering and Molecular Systems (NEMS)*, Xiamen, China, 2010.

[7] S. Y. Xiao, L. F. Che, X. X. Li and Y. L. Wang, "A novel fabrication process of MEMS devices on polyimide flexible substrates," *Microelectron. Eng.*, vol. 85, pp. 452–457, 2008.

[8] D. Resnik, D. Vrtačnik, M. Možek, B. Pečar and S. Amon, "Experimental study of heat-treated thin film Ti/Pt heater and temperature sensor properties on a Si microfluidic platform," *J. Micromech. Microeng.*, vol. 21, no. 2, p. 025025, 2011.

[9] D. Mager, V. Badilita, U. Loeffelman, P. J. Smith and J. G. Korvink, "Micro-MR coil construction by combining metal-on-glass inkjetting and MEMS techniques," in *Proc. Int. Soc. Mag. Reson. Med.*, West Yellowstone, USA, 2009.

[10] V. Demas, A. Bernhardt, V. Malba, K. L. Adams, C. Harvey, R. S. Maxwell and J. L. Herberg, "Electronic characterization of lithographically patterned microcoils for high sensitivity NMR detection," *J. Magn. Reson.*, vol. 200, pp. 56–63, 2009.

[11] S. Goto, T. Matsunaga, Y. Matsuoka, K. Kuroda, M. Esashi and Y. Haga, "Development of high-resolution intraluminal and intravascular MRI probe using microfabrication on cylindrical substrates," in *20th IEEE International Conference on Micro Electro Mechanical Systems (MEMS)*, Kobe, Japan, 2007.

[12] J.G. Kim, N. Takama, B.J. Kim and H. Fujita, "Optical-softlithographic technology for patterning on curved surfaces," *J. Micromech. Microeng.*, vol. 19, no. 5, p. 055017, 2009.

[13] K. Kratt, M. Seidel, M. Emmenegger, U. Wallrabe and J. G. Korvink, "Solenoidal micro coils manufactured with a wire bonder," in *21st IEEE International Conference on Micro Electro Mechanical Systems (MEMS)*, Tucson, USA, 2008.

[14] D. L. Olson, T. L. Peck, A. G. Webb, R. L. Magin and J. V. Sweedler, "High-resolution microcoil ^{1}H-NMR for mass-limited, nanoliter-volume samples," *Science*, vol. 270, pp. 1967–1970, 1995.

[15] Z. Yang, Y. Zhang and T. Itoh, "A flexible implantable microtemperature sensor on polymer capillary for biomedical applications", *26th International Conference on Micro Electro Mechanical Systems* (*IEEE MEMS 2013*), 2013.

[16] G. Fischer, H. Hoffmann and J. Vancea, "Mean free path and density of conductance electrons in platinum determined by the size effect in extremely thin films," *Phys. Rev. B*, vol. 22, no. 12, pp. 6065–6073, 1980.

[17] Z. Yang, Y. Zhang, T. Itoh and R. Maeda, "New fabrication method of three-electrode system on cylindrical capillary surface as a flexible implantable microneedle," *Surf. Rev. Lett.*, vol. 22, 1350027(8pp), 2013.

http://dx.doi.org/10.5772/66664

[18] Z. Yang, A. Toda, Y. Zhang, T. Itoh and R. Maeda. "An interventional flexible microneedle with three-electrode system on the capillary for continuous glucose monitoring and drug delivery", *2013 Transducers & Eurosensors XXVII: The 17th International Conference on Solid-State Sensors Actuators and Microsystems* (*TRANSDUCERS & EUROSENSORS XXVII*), 2013.

[19] H. Huang and C. Fu, "Different fabrication methods of out-of-plane polymer hollow needle arrays and their variations", *J. Micromech. Microeng.*, vol. 17, pp. 393–402, 2007.

[20] L. J. Fernández, A. Altuna, M. Tijero, G. Gabriel, R. Villa, M. J. Rodríguez, M. Batlle, R. Vilares, J. Berganzo and F. J. Blanco, "Study of functional viability of SU-8 based microneedles for neural applications", *J. Micromech. Microeng.*, vol. 19, p. 025007, 2009.

[21] A. Altuna, G. Gabriel, L. M. De La Prida, M. Tijero, A. Guimerá, J. Berganzo, R. Salido, R. Villa and L. J. Fernández, "SU-8-based microneedles for *in vitro* neural applications", *J. Micromech. Microeng.*, vol. 20, p. 064014, 2010.

[22] S. J. Moon and S. S. Lee, "A novel fabrication method of a microneedle array using inclined deep x-ray exposure", *J. Micromech. Microeng.*, vol. 15, pp. 903–911, 2005.

[23] M. Kimura, K. Bundo, Y. Imuro, Y. Sagawa and K. Setsu, "Chronoamperometry using integrated potentiostat consisting of poly-Si thin-film transistors", *IEEE Electron. Device Lett.*, vol. 32, pp. 212–214, 2011.

[24] J. D. Zahn, D. Trebotich and D. Liepmann, "Microdialysis microneedles for continuous medical monitoring", *Biomed. Microdevices*, vol. 7, pp. 59–69, 2005.

[25] S. Zimmermann, D. Fienbork, B. Stoeber, A. W. Flounders and D. Liepmann, in *12th International Conference on Solid-State Sensors, Actuators and Microsystems (Transducers'03)*, Boston, USA, 2003 99.

[26] K. E. Toghill and R. G. Compton, "Electrochemical non-enzymatic glucose sensors: A perspective and an evaluation", *Int. J. Electrochem. Sci.*, vol. 5, pp. 1246–1301, 2010.

IntechOpen